JOURNAL OF MATERIALS SCIENCE 19 (1984) 3873–3879

Effects of ageing after cathodic charging in austenitic stainless steels

P. ROZENAK, D. ELIEZER
Department of Materials Engineering, Ben-Gurion University of the Negev, Beer-Sheva, Israel

Ageing after cathodic charging resulted in a number of significant structural changes as the hydrogen diffused out of the specimen. The α'-phase is formed during hydrogen charging of the 316 steel. The weight fraction of the ϵ-martensite decreased with increasing ageing time. It is suggested that the $\epsilon \rightarrow \gamma$ transformation might be taking place during hydrogen release. Techniques for quantitative phase distribution in the stainless steel after various ageing times were used.

1. Introduction

The stability of the austenite in Fe–Ni–Cr stainless steels is affected by solute hydrogen and stress. Hydrogen-induced phase transformations in austenitic stainless steels have an h c p ϵ phase having varying lattice parameters as well as the b c c α' phase [1–3]. Using cathodic hydrogen charging, very high supersaturations of solute hydrogen can be achieved. Particularly in the surface layers of the alloy the hydrogen concentration is estimated to be about four orders of magnitude higher than its equilibrium value [2, 4, 5]. Ageing after cathodic charging resulted in a number of significant structural changes as the hydrogen diffused out of the specimen.

The purpose of this study is to examine the effects of hydrogen on the kinetics of phase transitions. Techniques for quantitative phase distribution in the stainless steel after various ageing times were used.

2. Experimental procedure

The studies were carried out on a 316-type austenitic stainless steel. The steel was of commercial grade, with the composition shown in Table I and was received in the form of sheets 0.1 mm thick. The grain size as measured by ASTM E-112 (1977) method was of the 2 number ASTM, obtained following 72 h at austenizing temperature. The hydrogen charging was performed at room temperature in 1 N H_2SO_4 solution with $0.25\,g\,l^{-1}$ $NaAsO_2$ added as a hydrogen recombination poison. A platinum counter electrode and a current density of $50\,mA\,cm^{-2}$ were used. A conventional Philips diffractometer equipped with step-motor, programmer, and teletype printer was used for the X-ray diffraction study. In diffractions with reflection (Bragg–Brentano) geometry only information from the thin surface layer of the flat sample is obtained. The intensity, I_t, of rays scattered by the surface layer of thickness t is equal to [16]:

$$I_t/I_\infty = 1 - \exp\left[-2\mu t/(\sin\theta)\right] \qquad (1)$$

where I_∞ is the intensity of rays scattered by an infinitely thick sample, μ is the linear absorption coefficient of the material, and θ is the Bragg angle. The thickness $t_{0.95}$, representing 95% of the total intensity of scattered rays, may be calculated from Equation 1 for various diffraction peaks and radiations. For the 111 austenite peak and radiations Cu$K\alpha$, Co$K\alpha$, Cr$K\alpha$ and Mo$K\alpha$ a value of $t_{0.95}$ equal to 2.6, 8.7 and 8.7 μm, respectively, was obtained. As reported elsewhere [6] the cracks after severe cathodic charging propagate inside the material to a depth approximately equal to 8 to 10 μm. It is essential to characterize this damage layer.

The weight fractions of the α' and ϵ-martensites present in the charged samples after various ageing times were determined using a method that employs various radiations (Cu$K\alpha$, Co$K\alpha$, Cr$K\alpha$

0022–2461/84 $03.00 + .12

TABLE I Chemical composition of 316 type austenitic stainless steel (wt %)

Cr	Ni	Mn	Si	C	Mo
17.98	12.09	1.71	1.879	0.05	2.08

and MoKα) and intensity measurements of various diffraction peaks [7].

3. Results and discussion

Cathodic charging of hydrogen into the austenitic stainless steels promoted diffraction peak shifts, line broadening, and the appearance of new reflections [1, 2, 8]. Typical results for the steel are shown in Fig. 1a for shallow penetrating CuKα radiation after cathodic charging: both α' and ϵ martensites were detected. The γ and ϵ phase reflections exhibit significant broadening and they are shifted to smaller 2θ values, consistent with the presence of a large hydrogen concentration gradient [9]. The $\epsilon(01\cdot1)$ peak overlapped a weak $\alpha'(1\,1\,0)$ martensite peak immediately after cathodic charging. The α' appeared after 40 min ageing, as the hydrogen diffused out of the specimen and the lattice parameter decreased, as indicated by the shifts of both the γ and ϵ reflections to larger 2θ values. On diffractograms in the early stage of ageing, splitting of γ; γ^* and ϵ; ϵ^* diffraction peaks was observed.

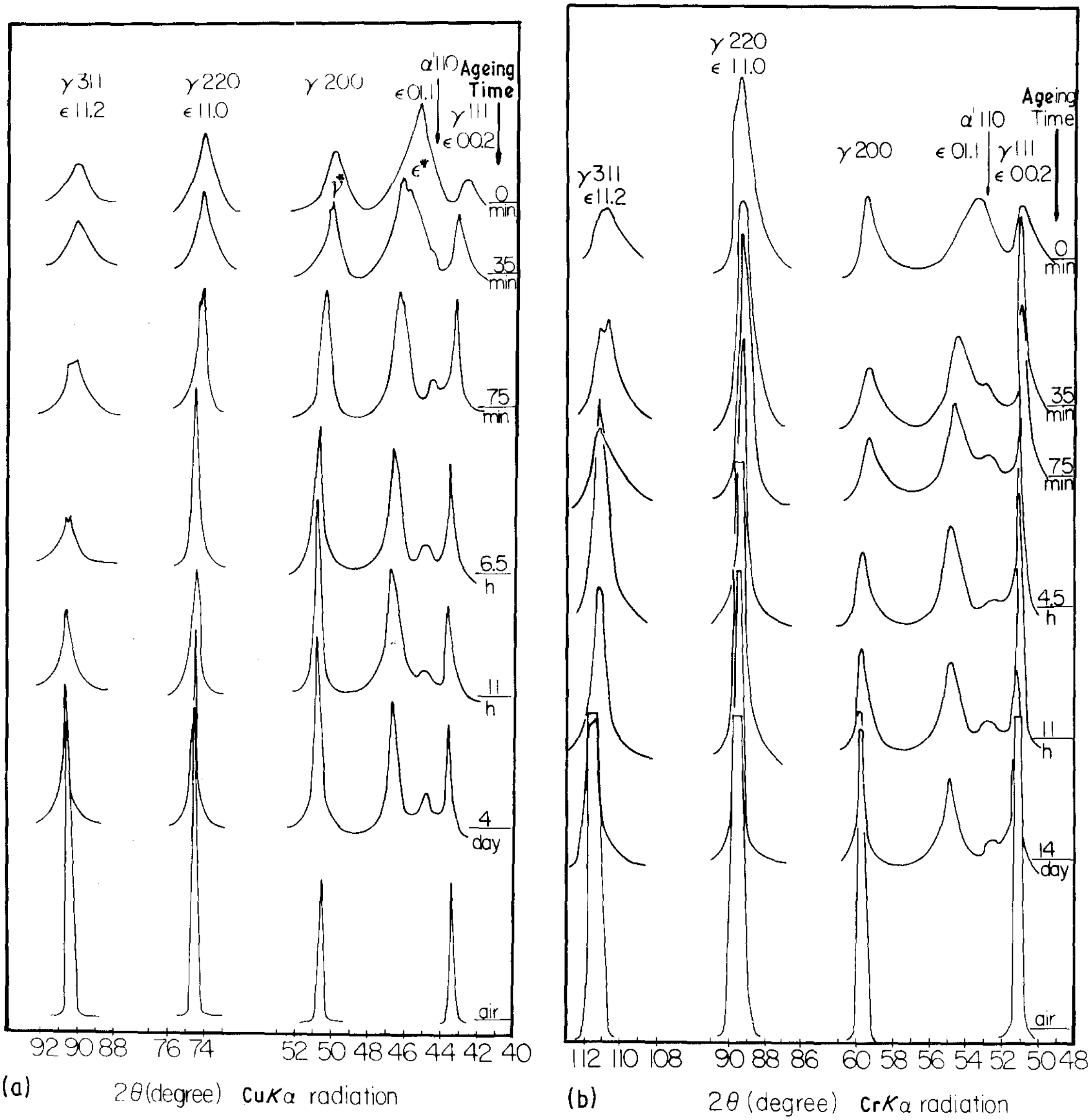

Figure 1 X-ray diffraction patterns after ageing times (originally 24 h, cathodically charged) for the times indicated. (a) CuKα radiation. (b) CoKα radiation. (c) CrKα radiation. (d) MoKα radiation.

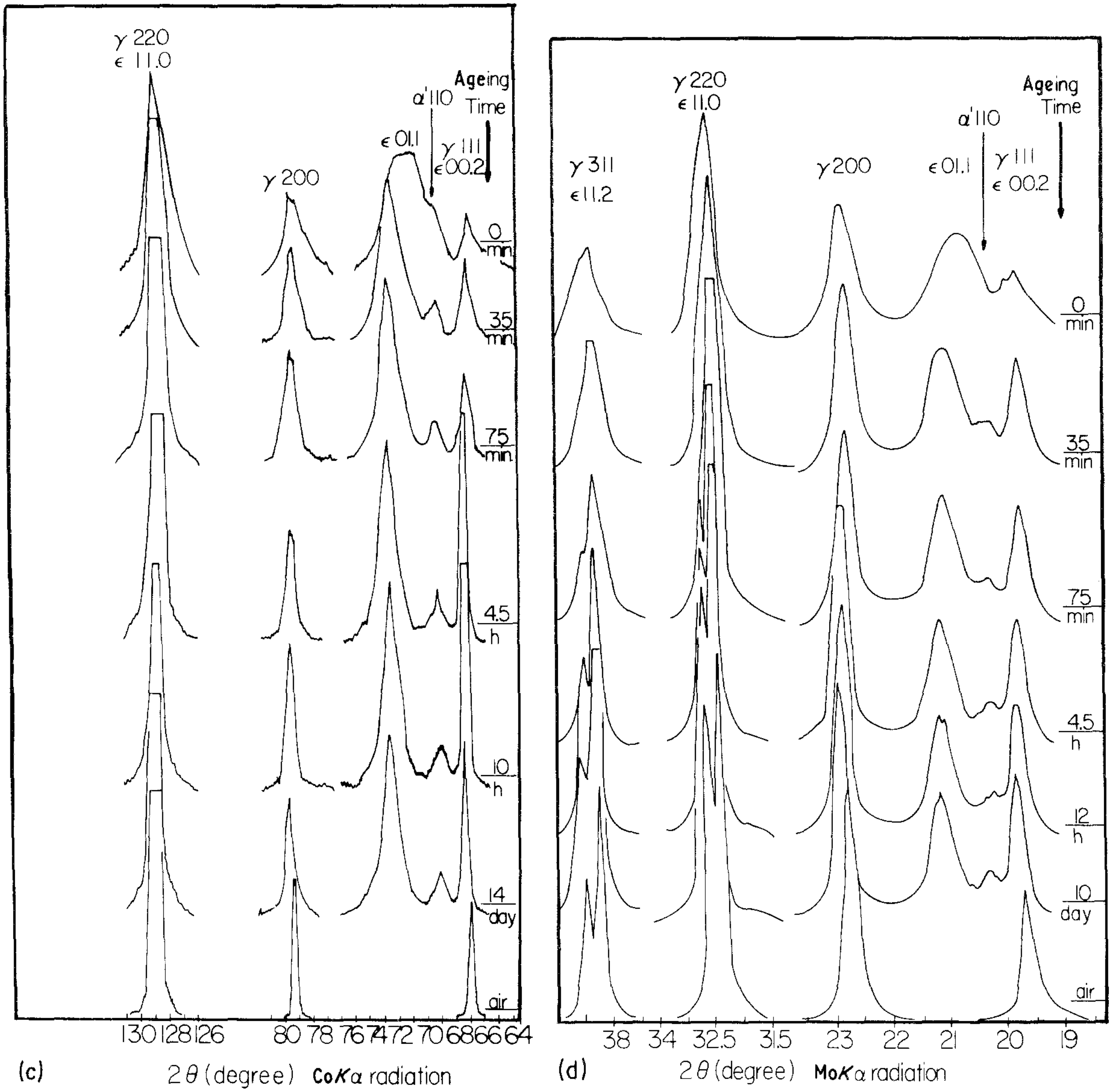

Figure 1 Continued.

After ageing the split peaks reformed into two singlets and shifted over to the regular position of the uncharged samples. This shift of ε-martensite and austenitic peaks is accompanied by decreasing peak width, and after ageing for 4 days the peak width is approximately the same as for the uncharged sample. The diffraction lines reflected from the hydrogenated layer are superimposed on those of the parent γ matrix, which are obviously increased if radiation of high Co*Kα*, Cr*Kα* or Mo*Kα* (Fig. 1b, c, d) penetration power is utilized. The weight fractions of martensitic phases were higher, when measured with Cu*Kα* radiation than when measured with the more deeply penetrating Co*Kα*, Cr*Kα* and Mo*Kα* radiations, suggesting that phases formed close to the specimen surface. Diffractograms obtained when Cr*Kα* high resolution radiation was used showed that the α′ phase appeared immediately after charging (Fig. 1c). The relative amounts of α′ phase remain stable after the charging in the steel. The α′(1 1 0) peak does not appear to shift during outgassing (Fig. 1a to d); its lattice parameter was equal to that reported for α′ formed by plastic deformation [8].

Fig. 2 demonstrates *d*-spacing relaxation behaviour during hydrogen release. The relaxation

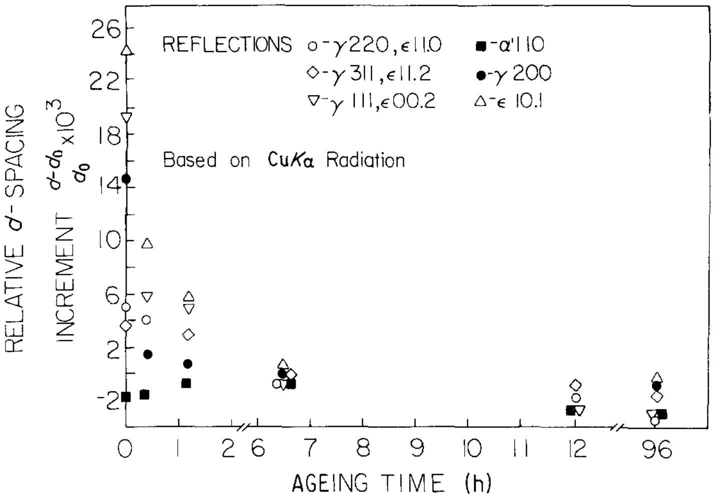

Figure 2 d-spacing relaxation curves (a plotted against time) during hydrogen release.

curves are plotted in terms of the d-spacing strains, $e = (d - d_0)/d_0$ against time, where d is the spacing of the reflecting planes during ageing after hydrogen charging, and d_0 is the spacing of the same planes of the uncharged samples (for ϵ- and α'-phase formed by plastic deformation). In our case the centroid of peaks was measured. Generally, the initial relaxation rate for the $\epsilon_{(10\cdot1)}$ reflection appeared higher than the $\epsilon_{(00\,2)}(\gamma\text{-}1\,1\,1)$ reflection and that for the $\gamma_{(2\,0\,0)}$ reflection. A lower relaxation rate was obtained for both $\epsilon_{(1\,1\cdot0)}(\gamma\text{-}2\,2\,0)$ and $\epsilon_{(1\,1\cdot2)}(\gamma\text{-}3\,1\,1)$ reflections. The centroid of the $\alpha'(1\,1\,0)$ peak found to be constant during the ageing process. In addition, negative d-spacing strains were obtained for the reflection peaks after relatively long relaxation times.

The quantitative X-ray method [7] is aimed at the analysis of phase distributions in thin surface layers comparable to the penetration depth of X-rays. The phase distribution can be modelled mathematically and the parameters of the distribution evaluated from diffraction data taken for various peaks and with various radiations. The distribution of the austenitic and ϵ-martensite in the surface layer of the steel is determined by:

$$\frac{I_{\gamma j}}{I_{0\gamma j}} = C_{0\gamma} + \frac{1 - C_{0\gamma}}{x_0}\,\frac{\sin\theta_{\gamma j}}{2\bar{\mu}} \times [1 - \exp(2\bar{\mu}x_0/\sin\theta_{\gamma j})] \quad (2)$$

$$\frac{I_{\epsilon j}}{I_{0\epsilon j}} = C_{0\epsilon} - \frac{C_{0\epsilon}}{x_0}\,\frac{\sin\theta_{\epsilon j}}{2\bar{\mu}} \times [1 - \exp(2\bar{\mu}x_0/\sin\theta_{\epsilon j})], \quad (3)$$

where j is the number of diffraction peak, $\bar{\mu}$ is the mean linear attenuation coefficient, $\theta_{\gamma(\epsilon)j}$ is the Bragg angle, $I_{\gamma(\epsilon)j}$ is the intensity of the austenite (ϵ-martensite) diffraction peak, $I_{0\gamma(\epsilon)}$ is the intensity for the pure austenitic (ϵ-martensitic) diffraction peak, x_0 is the phases definite depth, and $C_{0\gamma(\epsilon)}$ is the weight fraction of autenite (ϵ-martensite) on the surface of the specimen. The integral intensities of the austenitic peaks 1 1 1, 2 0 0, 2 2 0, 311 and ϵ-martensitic 00·2, 10·1, 11·0, 11·2 peaks were measured using $K\alpha$-radiations from Cr, Co, Cu, and Mo. The number of peaks analysed was 10 to 15.

An uncharged specimen provides $I_{0\gamma}$ intensities for a pure austenitic phase, since the ϵ-martensitic pure phase $I_{0\epsilon}$ was determined by the direct quantitative analysis comparison method [10]:

$$\frac{I_{\gamma j}}{I_{\epsilon j}} = \frac{R_{\gamma j}}{R_{\epsilon j}}\,\frac{C_{\gamma j}}{C_{\epsilon j}} \quad (4)$$

where R depends on $O_{\gamma(\epsilon)}$, Miller indices $h\,k\,l$, and the composition of substance. For pure phases, concentration $C_{0\epsilon}$ is equal to 1. The same methods were used for resolution of integral intensities of the austenitic peaks 1 1 1, 2 2 0 and 3 1 1 and for ϵ-martensitic from 0 0·2, 1 0·1 and 1 1·2 diffraction peaks.

The best parameters $C_{0\gamma(\epsilon)}$ and x_0 were found by minimalization of the sum:

$$\sum_{i=1}^{n}\,[(I_i/I_{0i})_{\text{calc}} - (I_i/I_{0i})_{\text{obs}}]^2$$

where $(I_i/I_{0i})_{\text{calc}}$ is calculated according to Equations 2 and 3, $(I_i/I_{0i})_{\text{obs}}$ are the observed values, and n is the number of measurements with various $\sin\theta_{\gamma(\epsilon)j/2\bar{\mu}}$ values.

Calculated relative intensity curves and experimental data after 35 min and 10 days ageing of the

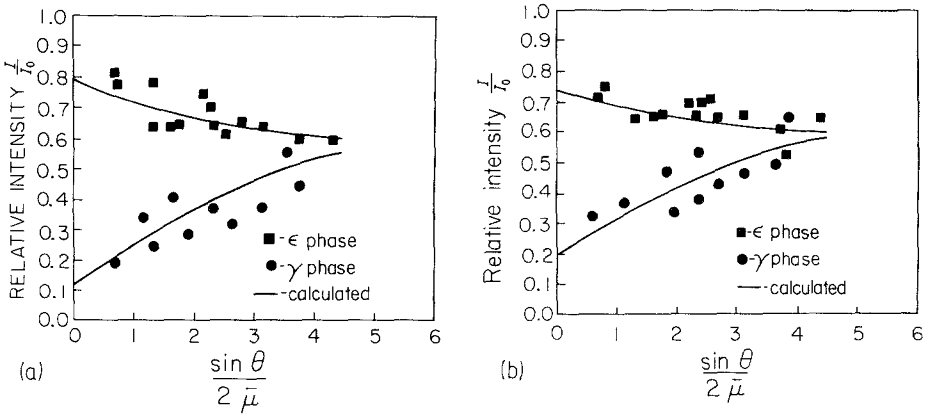

Figure 3 Calculated relative intensity curves and experimental data (24 h cathodic charged): (a) after 35 min ageing; (b) after 10 day ageing.

steel which had been cathodically charged for 24 h, are shown in Figs. 3a and b. The best fit parameters were found to be $C_{0\gamma} = 0.14$, $C_{0\epsilon} = 0.79$ and $C_{0\gamma} = 0.20$, $C_{0\epsilon} = 0.73$ for 35 min and 10 day aged steel, respectively. The mean square deviation of the $(I_i/I_{0i})_{\text{obs}}$ from the best fit is equal to 0.1150 when $x_0 = 7\,\mu\text{m}$. The weight fraction value of the α'-martensite $C_{0\alpha'}$, was found from the relation:

$$C_{0\gamma} + C_{0\epsilon} + C_{0\alpha'} = 1 \qquad (4)$$

The most striking result of these studies is the instability of the γ-phase induced by severe cathodic charging of hydrogen into what is normally considered to be stable stainless steel. In the uniform solid solution, the intensity of the diffraction peaks decreases due to local lattice distortion, but the peaks themselves remain sharp. The reason for peak broadening (Fig. 1) is the formation of non-uniform solid solution of hydrogen in austenite. Since both hydrogen penetration during charging and hydrogen release during ageing are diffusion controlled, large concentration gradients in the thin surface layer of depths comparable with the X-ray penetration depth are expected. During the ageing process, hydrogen loss is expected primarily through the external surface. The hydrogen concentration during ageing is quickly reduced to low values at the surface, reaches a peak just below the surface, and then decreases at greater depths [8, 9]. Actually, the hydrogen concentration is non-uniform within a single grain and this results in non-uniform expansion, which leads to the development of the internal stresses [6]. As the internal stresses would be expected to increase with charging time then stress relaxation should consequently occur; evidence of such relaxation is crack formation as shown in Fig. 4.

The distribution of the retained ϵ and α' martensites in the surface layer of the steel after charging for 24 h is shown in Figs. 5a and b. The fraction of ϵ-martensite drops from about 79% on the surface to zero at a depth of approximately 7 μm, for samples aged for 35 min while the amount of α'-phase decreased from about 7% on the surface to zero at the depth of approximately 7 μm below the surface (Fig. 5a). The amount of ϵ in this type of steel decreased after long (10 day) ageing times to about 73%, and the α'-phase because stable (at about 6.7%) on the surface (Fig. 5b). Thus, the information leads us to suggest that the $\epsilon \rightarrow \gamma$ phase transition occurred during outgassing of hydrogen-charged stainless steel.

The phase transition induced by cathodic

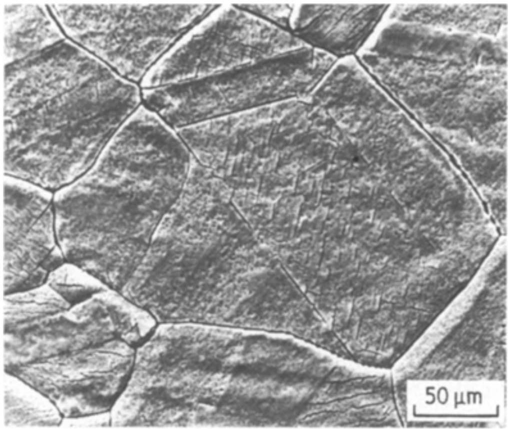

Figure 4 Scanning electron micrographs of surface cracks formed in 316 type specimens after 24 h cathodic charging.

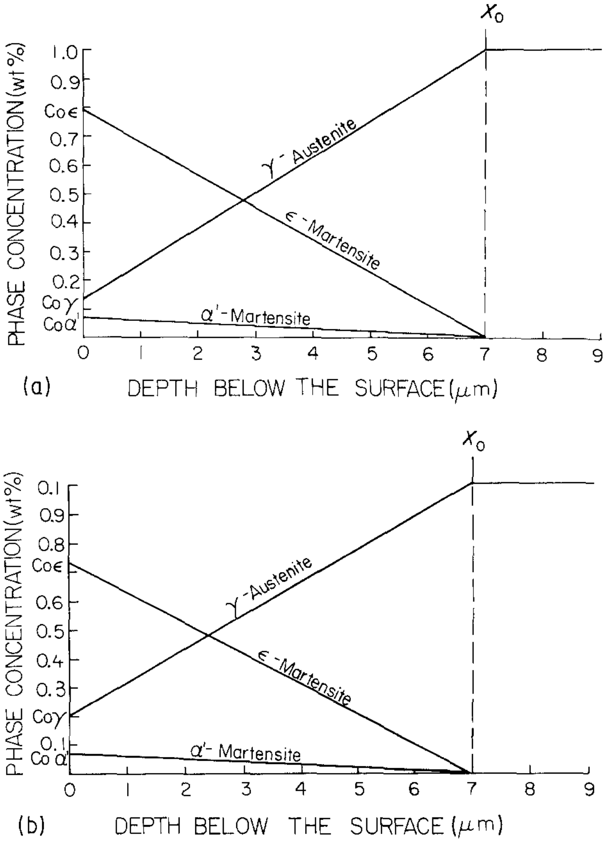

Figure 5 Phases distribution in surface layers in 316 stainless steel cathodically charged: (a) after 35 min ageing; (b) after 10 day ageing.

charging of stainless steel suggests that both the hydrogen concentration and stress states in the near-surface region must be considered to play significant roles. The effect of hydrogen on the γ-phase stability is to decrease the γ-phase stability and possibly to induce transformation of the γ-phase to α'- or ε-martensite [1–3, 8]. As shown in Fig. 1, significant transformation of γ to ε (about 79%), measured after 35 min, occurred after charging of the type 316 steel.

High hydrogen concentration corresponds to about 2.5% linear spacing strain of the 10·1 ε-phase plane, similar to the 111 austenite plane strained to about 2%, in agreement with the peak shifts after cathodic charging (Fig. 2). This high hydrogen concentration decreases to low values at the surface during ageing, and the lattice parameters approach values of the original γ and ε phases. Narita *et al.* [2] have suggested that the stainless steel –H system appears to have a miscibility gap in which the γ-phase, containing about 21% H, is in equilibrium with the γ^* phase, containing about 55% H; this is in contrast to the typical continuous nature of lattice contraction of the γ^* during relaxation that has been confirmed experimentally by Mathias *et al.* [11]. It seems that the appearance of γ and γ^* as well as ε and ϵ^* is a result of a very special hydrogen distribution. In contrast to this, the zero shift in the α'-phase peak suggests that the α'-phase absorbs far less hydrogen than γ and ε phases as a result of cathodic charging. It is proposed that the ε was formed from the γ-matrix by a process of overlapping stacking faults on each alternative $\{111\}_\gamma$ plane [1, 12, 13], arising from a decrease in stacking fault energy by dissolved hydrogen. This phenomenon, as well as the thinness of the ε-phase plates, is the reason for the retention of the broadened ε-peaks even after prolonged ageing. The ε-phase is generated in the thin (~ 7 μm) surface layer of the samples. This layer is characterized by a hydrogen concentration gradient and the development of high tensile surface stresses.

The weight fraction of the ε-martensite decreased (to about 6%) with increasing ageing time (after 10 days). On the other hand, the amount of α'-phase was unaffected and it is suspected that the ε → γ transformation might be taking place during hydrogen release. In the present experiments and as previously reported [1, 2, 14], cathodic charging of type 316 led to surface cracking which was both transgranular and intergranular. This is consistent with the expectation of high tensile stresses during charging and ageing [6]. Cracks extended to depths of about 10 μm after 24 h cathodic charging. The depth of the cracking corresponded to the depth of the distribution of phase transitions estimated by a quantitative method. In the case of type 304 steel, which was severely embrittled by hydrogen pre-charging, it has been shown that cracks propagated mainly along the ϵ-martensite phase and partly in the region having a mixed structure of α' and ϵ-martensite phases [15].

4. Conclusions

1. The γ-phase stability is affected by solute hydrogen and stress. Transformation of the f c c γ to the h c p ϵ and b c c α' phases, and the appearance of γ^*, as well as ϵ^* is a result of a very special hydrogen distribution after hydrogen charging and during outgassing after charging.

2. The α'-phase was formed during hydrogen charging of 316 steel. No evidence of the α'-phase shift during ageing after charging was found.

3. The weight fraction of the ϵ-martensite decreased with increasing ageing time. On the other hand, the amount of α'-phase was unaffected. It is suggested that the $\epsilon \rightarrow \gamma$ transformation might be taking place during hydrogen release.

References

1. M. L. HOLZWORTH and H. R. LOUTHAN JR, *Corrosion* **24** (1968) 110.
2. N. NARITA, C. J. ALTSTETTER and H. K. BIRNBAUM, *Met. Trans.* **13A** (1982) 1355.
3. S. TAHTINEN, J. KIVILAHTI and H. HANNINEN, in Proceedings of the 3rd International Conference on Hydrogen and Materials, Paris, edited by P. Azov (June, 1982) p. 185.
4. M. R. LOUTHAN and R. G. DERRICK, *Corros. Sci.* **15** (1975) 565.
5. K. FARRELL and M. B. LEWIS, *Scripta Metall.* **15** (1981) 661.
6. P. ROZENAK, L. ZEVIN and D. ELIEZER, *J. Mater. Sci. Lett.* **2** (1983) 63.
7. L. ZEVIN, P. ROZENAK and D. ELIEZER, *J. Appl. Cryst.* **17** (1984) 18.
8. P. ROZENAK, L. ZEVIN and D. ELIEZER, *J. Mater. Sci.* **19** (1984) 567.
9. A. ATRENS, J. J. BELLINA, N. F. FIORE and R. J. COYLE, "Proceedings of the Symposium on the Metals Physics of Stainless Steels", Denver, 1978, edited by E. Collings and H. King (AIME, New York, NY, 1979) p. 54.
10. B. D. CULLITY, "Element of X-ray Diffraction" (Addison Wesley, Massachusetts, 1967) p. 391.
11. H. MATHIAS, Y. KATZ and S. NADIV, *Met. Sci.* **12** (1978) 129.
12. J. M. RIGSBEE, *Metallogr.* **11** (1978) 493.
13. E. MINKOVITZ, M. TALIANKER and D. ELIEZER, *J. Mater. Sci.* **16** (1981) 2507.
14. D. ELIEZER, D. G. CHAKRAPANI, C. J. ALTSTETTER and E. N. PUGH, *Met. Trans.* **10A** (1979) 935.
15. T. NAKAYAMA and M. TAKANO, *Corrosion-Nace* **38** (1982) 1.
16. H. P. KLUG and L. E. ALEXANDER, "X-ray Diffraction" (John Wiley, New York, 1974) p. 360.

Received 8 July 1983
and accepted 13 January 1984